FEBS Letters

FEBS PRESS science publishing by scientists

Regulation of Tip60-dependent p53 acetylation in cell fate decision

Ping Wang[1], Han Bao[2], Xiao-Peng Zhang[2], Feng Liu[1] and Wei Wang[1]

1 National Laboratory of Solid State Microstructures and Department of Physics, Nanjing University, China
2 Kuang Yaming Honors School, Nanjing University, China

Correspondence
X.-P. Zhang, Kuang Yaming Honors School, Nanjing University, Nanjing 210023, China
E-mail: zhangxp@nju.edu.cn
and
F. Liu, National Laboratory of Solid State Microstructures and Department of Physics, Nanjing University, Nanjing 210093, China
E-mail: fliu@nju.edu.cn

(Received 17 June 2018, revised 30 October 2018, accepted 31 October 2018, available online 26 November 2018)

doi:10.1002/1873-3468.13287

Edited by Angel Nebreda

The acetylation of p53 plays an essential role in regulating its transcriptional activity. Nevertheless, how p53 acetylation is modulated in cell fate decision is less understood. We developed a network model to reveal how Tip60-dependent p53 acetylation is regulated to modulate cellular outcome. We proposed that p53 is progressively activated and exhibits distinct dynamics depending on the severity of DNA damage. For mild damage, p53 is primarily activated to trigger cell cycle arrest by transactivating p21, with its concentration showing pulses. For severe damage, p53 is acetylated at Lysine 120 (K120) by Tip60 to trigger apoptosis by inducing PUMA, and its concentration increases to high levels. Several p53-centered feedback loops coordinate to regulate its acetylation status, ensuring a robust decision on cell fate.

Keywords: cell fate decision; network model; numerical simulation; p53 acetylation; Tip60

p53 plays a key role in tumor suppression by maintaining genomic integrity. It mainly acts as a transcription factor, modulating gene expression to induce cell cycle arrest and apoptosis [1]. In unstressed cells, p53 is kept at a very low level due to degradation by its negative regulator Mdm2, which is induced by p53 and acts as a ubiquitin E3 ligase [2]. Upon DNA damage, p53 is released from Mdm2 inhibition by post-translational modifications including phosphorylation and acetylation [3]. p53 can be primarily phosphorylated at Ser15/20 to induce cell cycle arrest, and its further phosphorylation at Ser46 may promote apoptosis [4,5]. Moreover, p53 phosphorylation at N-terminus promotes the sequential acetylation of p53. For example, p53 phosphorylation at Ser15 facilitates its acetylation in the C-terminal [6], and Ser46 phosphorylation is required for p53 acetylation at Lysine 382 (K382) in apoptosis induction [7]. It is significant to further explore how p53 acetylation is regulated in the DNA damage response (DDR).

It has been established that p53 acetylation is indispensable for its transcriptional activity [8]. Upon DNA damage, several residues in the C-terminal domain of p53 are acetylated by the acetyltransferases p300/CBP or p300/CBP-associated factor, contributing to its sequence-specific DNA binding. K120 in the DNA-binding domain of p53 is acetylated by Tip60 [9,10]. Tip60 is required for induction of both p21 and p53 upregulated modulator of apoptosis (PUMA), while K120 acetylation is only crucial for *puma* expression [8]. On the other hand, the phosphorylation of Tip60 at Ser86 by glycogen synthase kinase 3 (GSK3) is required for p53-dependent PUMA induction and apoptosis in the DDR [11]. But GSK3 can be deactivated *via* AKT-mediated phosphorylation in the presence of growth factors [12], which tends to inhibit Tip60 activity and

Abbreviations
DDR, DNA damage response; DSBs, double-strand breaks; GSK3, glycogen synthase kinase 3; HB, Hopf bifurcation; NFL, negative feedback loop; ODEs, ordinary differential equations; PFL, positive feedback loop; SN, saddle-node; UV, ultraviolet.

promote cell survival [11]. It is worthy to determine how Tip60 activity is dynamically regulated in the DDR.

p53 dynamics play a key role in cell fate decision. The p53 level exhibits distinct dynamic modes depending on the cell and stress types [13]. For example, uniform pulses can be evoked upon ionizing radiation, whereas only a dosage-dependent single pulse appears in response to ultraviolet (UV) radiation. Furthermore, cell fates are tightly controlled by p53 dynamics, and perturbing the dynamic mode of p53 may be a potential approach for cancer therapy [14,15]. A series of models have been developed to explore the mechanism for cell fate decision by p53 in the DDR [16–20]. However, most of them focused on the role of p53 phosphorylation in regulating its activity, and the role of p53 acetylation was seldom considered. It is essential to unravel the effects of acetylation on p53 dynamics and cellular output.

Here, we developed a model of cellular signaling to investigate how Tip60-dependent p53 acetylation is regulated to ensure a reliable cell fate decision upon DNA damage. Simulation results show that p53 dynamics are shaped by several p53-centered negative and positive feedback loops. p53 undergoes pulsing, two-phase dynamics or monotonic increasing, depending on the severity of DNA damage. Apoptosis induction is regulated by the p53-phosphatase TENsin homolog (PTEN)-AKT-GSK3-Tip60 positive feedback loop in which p53 induces PTEN to repress AKT activity, thereby activating Tip60-mediated p53 acetylation at K120. We analyzed the intricate relationships among AKT, PTEN, GSK3 and Tip60 and their influence on cellular outcome. Our work may provide a theoretical framework to further probe the mechanism of DDR mediated by p53.

Materials and methods

Model

In this work, we built an integrated model for the p53 network in response to DNA damage induced by etoposide treatment, focusing on the regulation of p53 acetylation by Tip60. The model characterizes p53 activation, regulation of p53 acetylation, and cell fate decision (Fig. 1). Four important feedback loops are considered, that is, p53-Mdm2, ATM-p53-wild-type p53-induced phosphatase 1 (Wip1), p53-PTEN-AKT-Mdm2 and p53-PTEN-AKT-GSK3-Tip60 loops. The details of the model are presented as follows.

Activation of p53 by DNA damage-mediated ATM activation

As a type of anticancer drug, etoposide mainly induces double-strand breaks (DSBs) in DNA. The severity of DNA damage is denoted by S_D. DNA repair is omitted here since etoposide treatment produces DNA damage persistently. As a sensor of DSBs, ATM is activated to the phosphorylated monomeric form ATM* (Eqns 1,2 in Supporting Information). ATM* can phosphorylate both p53 and Mdm2, leading to the degradation of Mdm2 and activation of p53 (Eqns 4,5 and 14). Given p53 is mostly in the nucleus, the role of cytoplasmic p53 is ignored. Mdm2 can be phosphorylated by AKT, promoting its nuclear entry to degrade p53 [21]. Dephosphorylated and phosphorylated Mdm2 are denoted by Mdm2 and Mdm2* respectively, and their conversion is characterized by the Michaelis-Menten kinetics (Eqns 13,14).

Regulation of p53 acetylation and cell fate decision

Based on its modification status, activated p53 (p53*) is divided into $p53_{acp}$, $p53_{acf}$ and $p53_{acc}$. $p53_{acp}$ is primarily phosphorylated in the N-terminal and acetylated in the C-terminal [6]. $p53_{acf}$ is further phosphorylated at Ser46 based on $p53_{acp}$. $p53_{acc}$ is the completely active form of p53 that is further acetylated at K120 specifically by Tip60 [10]. $p53_{acp}$ is activated by ATM-dependent phosphorylation and acetylation [22–24], and it subsequently induces Wip1 to inactivate ATM through dephosphorylation, enclosing a negative feedback loop (NFL) required for the recurrent activation of p53 [25] (Eqns 2–5, 15 and 16). p53DINP1 promotes phosphorylation of p53 at Ser46 [5], contributing to accumulation of $p53_{acf}$ (Eqn 6). It is assumed that p53DINP1 is induced by all activated forms of p53 [5] (Eqns 10,11). Tip60 promotes the conversion from $p53_{acf}$ to $p53_{acc}$ [10], characterized by the Michaelis-Menten kinetics (Eqn 7). The acetyltransferase activity of Tip60 is activated by GSK3 *via* phosphorylation at Ser86 [11], and Tip60 is divided into active Tip60* and inactive Tip60. Since GSK3 is deactivated by AKT *via* phosphorylation [12], we consider two forms of GSK3: inactive GSK3 (phosphorylated) and active GSK3* (dephosphorylated). Given that phosphorylation is the main regulation mode for Tip60 and GSK3 in U2OS cells in the DDR [11], the total levels of Tip60 and GSK3 are assumed to be constant and are denoted by $Tip60_{tot}$ and $GSK3_{tot}$, respectively. The enzymatic reactions for GSK3 and Tip60 (de)phosphorylation are characterized by the Michaelis–Menten kinetics (Eqns 23,25).

A positive feedback loop (PFL) is involved in the regulation of p53 acetylation by Tip60. It is assumed that both $p53_{acf}$ and $p53_{acc}$ can promote *pten* transcription since phosphorylated p53 at Ser46 selectively induces *pten* [26] (Eqn 17). As a result, PTEN deactivates AKT by promoting the conversion from phosphatidylinositol 3,4,5 phosphate (PIP3) to phosphatidylinositol 4,5 phosphate (PIP2) [27], and AKT-mediated nuclear entry of Mdm2 is repressed [21], thereby stabilizing p53 [27]. Meanwhile, GSK3 and Tip60 are

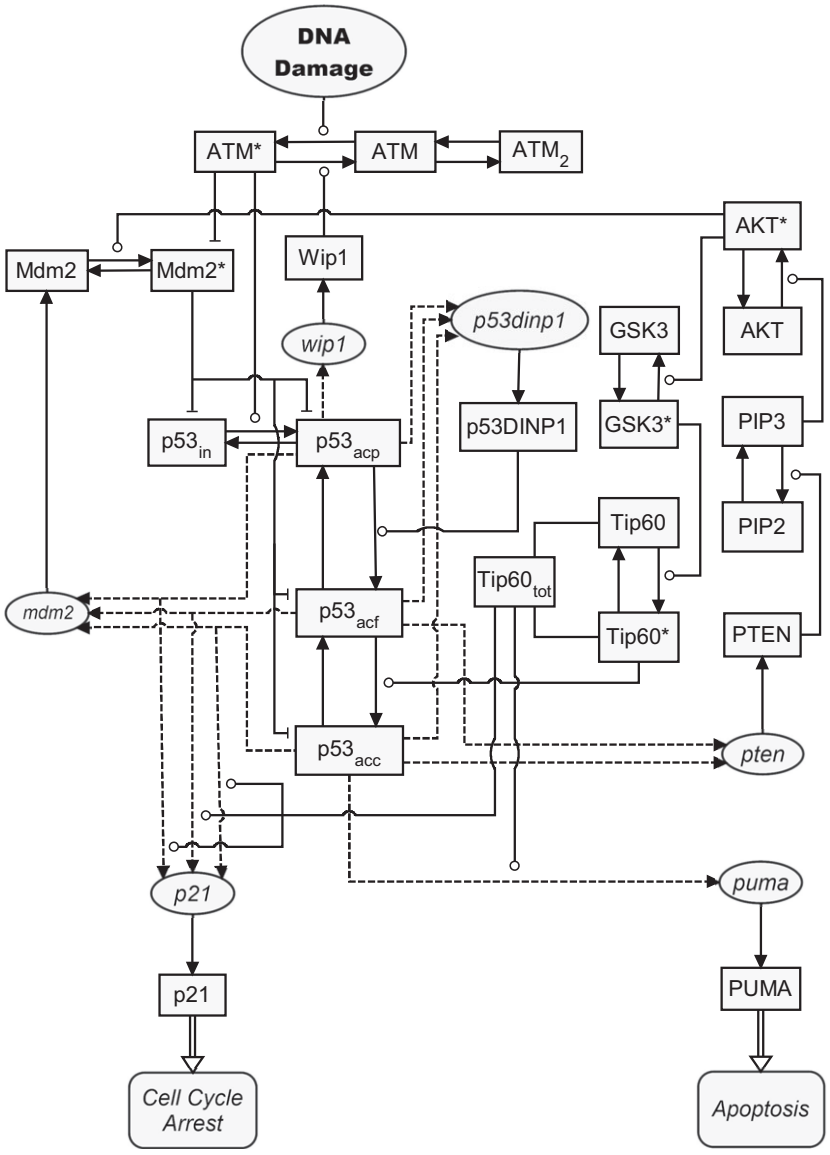

Fig. 1. Schematic of the integrated model. The model comprises the classic p53-Mdm2 negative feedback loop, p53-PTEN-AKT-Mdm2 and p53-PTEN-AKT-GSK3-Tip60 positive feedback loops. p21 and PUMA are downstream effectors of p53, activating cell-cycle arrest and apoptosis, respectively. The transactivation of genes by p53 is indicated by arrow-headed dotted lines. Translation from mRNAs to proteins and interactions between proteins are denoted by solid lines. Circle- and bar-headed lines denote promotion and repression, respectively.

sequentially activated to facilitate p53 acetylation at K120. As the total level of AKT (AKT_{tot}) is nearly unchanged in the DDR [28], it is assumed to be constant. The conversion from AKT to AKT* is controlled by PIP3-dependent phosphorylation. For simplicity, the total level of PIP2 and PIP3, PIP_{tot}, is also considered a constant. The reversible phosphorylation of AKT and PIP3 is described by the Michaelis-Menten kinetics (Eqns 19 and 21).

It has been verified that Tip60 is required for p53-dependent *p21* induction, and p53 acetylation at K120 is crucial for *puma* induction [10]. Consequently, it is assumed that all the three forms of p53* can induce *p21* expression, while only $p53_{acc}$ can transactivate *puma* [10]. Given Tip60 acts as a coactivator for p53-dependent *p21* and *puma* expression [10], the transcription rate of both *p21* and *puma* is proportional to $Tip60_{tot}$. Hill function is exploited to describe the transcription of p53-targeted genes, and the Hill coefficient is set to 2 since p53 is mostly present in dimers and then binds to DNA in tetrameters [29]. For simplicity, the translation processes from these mRNA transcripts to corresponding proteins are depicted by mass action kinetics. It is assumed that high expression of p21 and PUMA induces cell cycle arrest and apoptosis, respectively.

Methods

The details of model construction and parameter setting are presented in Supporting Information. The dynamics of all components in the model are characterized by ordinary

differential equations (ODEs) in Method S1. [·] denotes the concentration of each species. The initial concentration of each species was set to its steady-state value at $S_D = 0$ (Table S1). All parameter values are listed in Table S2. The software OSCILL8 was used to numerically solve the ODEs and plot bifurcation diagrams.

All the simulation results were based on the deterministic ODEs except Figs 4 and 8. To validate the model, we compared the average concentrations of the proteins over a population of 5000 cells with experimental data from western blot. Considering that p53 dynamics show remarkable variability between individual cells even exposed to the same dose of DNA damaging agent, it was assumed that S_D obeys a Poisson distribution with a mean of S_{Dave} in the population of cells.

Results

Cell fate decision guided by p53 dynamics

We first show the typical dynamics of [$p53_{acp}$], [$p53_{acf}$], [$p53_{acc}$], [p21] and [PUMA] in response to DNA damage (Fig. 2). Upon mild damage ($S_D = 15$), $p53_{acp}$ dominates in the three forms of p53* with its concentration undergoing persistent pulses, and only a small fraction of p53 is acetylated at K120 (Fig. 2A). Thus, [p21] tightly follows the behavior of p53 and exhibits pulses, whereas [PUMA] remains at basal levels (Fig. 2B). Consequently, cell-cycle arrest is induced.

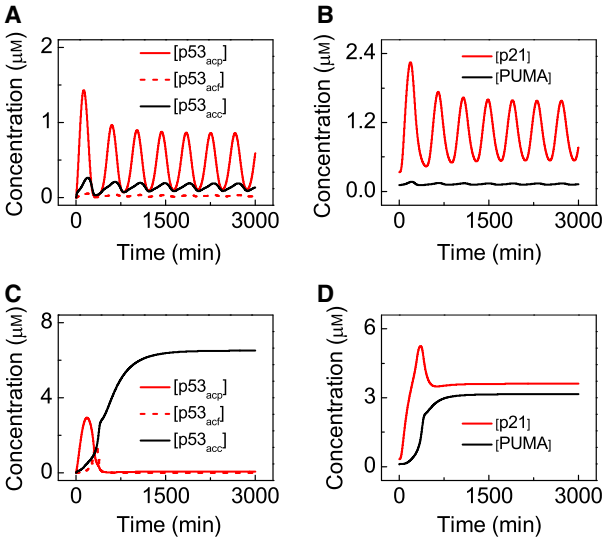

Fig. 2. p53 dynamics and cellular outcome for distinct DNA damage. (A,B) Time courses of [$p53_{acp}$] (red, solid), [$p53_{acf}$] (red, dash) and [$p53_{acc}$] (black) (A), and [p21] (red) and [PUMA] (black) (B) for $S_D = 15$. (C,D) Time courses of [$p53_{acp}$] (red, solid), [$p53_{acf}$] (red, dash) and [$p53_{acc}$] (black) (A), and [p21] (red) and [PUMA] (black) (B) for $S_D = 130$.

Upon severe damage ($S_D = 130$), [$p53_{acp}$] and [$p53_{acf}$] take turns undergoing a single pulse, and [$p53_{acc}$] rises toward a high plateau and becomes predominant finally (Fig. 2C). As a result, [p21] settles at high levels after a single pulse due to the dynamic behavior of $p53_{acp}$, while [PUMA] attains its high levels after a delay owing to the dynamics of $p53_{acc}$ (Fig. 2D). Apoptosis is induced by PUMA to eliminate the cell. These results agree well with the bimodal dynamics of p53 observed experimentally, that is, p53 pulsing with low amplitudes triggers cell-cycle arrest, whereas monotonic increasing of p53 leads to apoptosis [15]. Taken together, p53 dynamics control cellular output [14].

Various modes of p53 dynamics

With the default parameter setting, p53 can undergo five kinds of behaviors, depending on the extent of DNA damage (Fig. 3A). Besides two behaviors shown in Fig. 2, the total concentration of active p53, [p53*], can remain at low or intermediate levels after damped oscillations, or rise to high levels with varying delays. Accordingly, distinct cellular outcomes are evoked. Upon sublethal damage ($S_D = 15$ or 55), both p53 pulsing and sustained p53 activation can induce senescence, although it takes a much longer time in the former case [14]. At $S_D = 65$, [p53*] gradually switches to high levels after damped oscillations (termed two-phase dynamics) [19,30]; in contrast, [p53*] rises quickly toward high levels after a small pulse upon extremely severe damage ($S_D = 130$) [15]. Together, the intensity of DNA damage is encoded by the modes of p53 dynamics in the cellular response.

Bifurcation analysis reveals the dependence of steady-state p53* levels on S_D. There are two saddle-node (SN) and two Hopf bifurcation (HB) points in Fig. 3B. Conversion between the low and high expression of p53 is realized *via* bistable switching. Only when S_D exceeds the critical value at SN_1 can [p53*] switch to high levels. Around the lower unstable steady states, the oscillation region is constrained by HB_1 and HB_2. Clearly, the long-term dynamic behaviors of [p53*] in the figures above well coincide with these features.

Next, the significance of the ATM-p53-Wip1 NFL for p53 pulsing is tested. The p53-dependent transcription rate of *wip1*, k_{swip1}, can modulate the intensity of the NFL. [$p53_{acp}$] pulsing sustains persistently with $k_{swip1} = 0.008$, but becomes damped and even disappears with decreasing k_{swip1} (Fig. 3C). The bifurcation diagrams of [$p53_{acp}$] versus S_D show distinct properties for $k_{swip1} = 0$ and 0.008 (Fig. 3D). Cutting off the

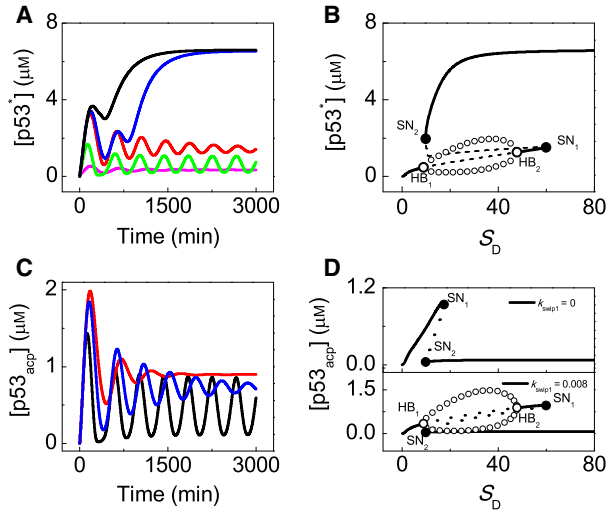

Fig. 3. Dynamic modes of p53 depending on the severity of DNA damage. (A) Shown are low-amplitude damped oscillation (magenta, $S_D = 5$), pulsing (green, $S_D = 15$), high-amplitude damped oscillation (red, $S_D = 55$), two-phase dynamics (blue, $S_D = 65$) and monotonic increasing (black, $S_D = 130$) of [p53*]. (B) Bifurcation diagram of [p53*] versus S_D. The stable and unstable steady states are denoted by solid and dashed lines, respectively. The open circles denote the maximum and minimum of oscillation. (C) Time courses of [p53$_{acp}$] at $S_D = 15$ for $k_{swip1} = 0.008$ (black), $k_{swip1} = 0.001$ (blue) and $k_{swip1} = 0$ (red). (D) Bifurcation diagram of [p53$_{acp}$] versus S_D for $k_{swip1} = 0.008$ (bottom) and $k_{swip1} = 0$ (upper).

NFL by setting $k_{swip1} = 0$ not only shortens the upper steady-state branch but eliminates two HBs on it. Therefore, the ATM-p53-Wip1 NFL is indeed required for the production of recurrent p53 pulses in response to DNA damage, consistent with the existing experimental observation [25].

To validate the theoretical modeling, it is necessary to compare simulation results with the corresponding experimental data. To compare with the experimental data from western blot [15], we take the average of p53$_{tot}$ over a population of cells. For convenience, the maximum of [p53$_{tot}$] (the total concentration of p53) upon $S_{Dave} = 130$ is assumed to be comparable to that of [p53] in cells treated with 100 μM etoposide [15], and both the maxima are set to 1 (Fig. 4). At $S_{Dave} = 15$, [p53$_{tot}$] from the simulations is much lower than 1, coinciding well with time courses of [p53] upon 1 μM etopside in U2OS cells [15]. At $S_{Dave} = 130$, [p53$_{tot}$] rises to high levels after a small pulse, agreeing fairly well with the dynamics of p53 in cells treated with 100 μM etoposide in the same cell line [15]. Together, our model can reproduce the p53 dynamics at the population level for both low and high DNA damage.

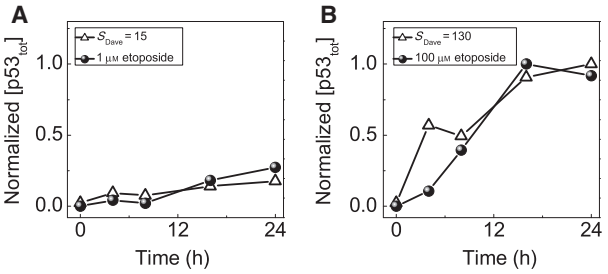

Fig. 4. Comparison of simulation results with experimental data. Time courses of normalized [p53$_{tot}$] upon mild (A) and severe DNA damage (B). The lines with sphere denote the experimental data from U2OS cells exposed to 1 and 100 μM etoposide [15], and the lines with triangle denote the simulation results for S_{Dave} = 15 and 130.

Repression of p53 acetylation at K120 by AKT

We have shown that acetylation of p53 at K120 is required for the induction of PUMA and apoptosis. It is worthy to systematically explore how p53 acetylation is modulated, depending on the severity of DNA damage and Tip60 activity. It has been reported that both AKT and GSK3 affect p53 acetylation at K120 by regulating Tip60 activity [11]. In the following, we will reveal how AKT affects the p53-mediated cell fate decision.

Experimentally, AKT activity is repressed when U2OS cells are treated with PI3K inhibitor that prevents the conversion from PIP2 to PIP3 [11]. We mimic the effect of PI3K inhibitor on AKT activity by modulating the phosphorylation rate of PIP2, k_{acPIP2}. The curves of [AKT*] dynamics largely move upward with increasing k_{acPIP2} (Fig. 5A). The bifurcation diagram of [AKT*] versus k_{acPIP2} further reveals the positive correlation between [AKT*] activity and k_{acPIP2} (Fig. 5B). Thus, it is feasible to repress AKT activity by adding PI3K inhibitor.

Upon severe DNA damage ($S_D = 65$), [p53$_{acc}$] exhibits two-phase dynamics or monotonic increasing with varying k_{acPIP2} (Fig. 5C). When AKT* is insufficient (e.g., $k_{acPIP2} = 0$ or 3), [p53$_{acc}$] rises to high levels rather quickly; conversely, increasing k_{acPIP2} slows down the accumulation of p53$_{acc}$ and prolongs the delay for complete activation of p53. When k_{acPIP2} is sufficiently large ($k_{acPIP2} = 10$), [p53$_{acc}$] remains at low levels. Thus, cells can be rescued from apoptosis by preventing p53 from activation when the abundance of AKT* is significantly enhanced.

AKT exploits two pathways to inhibit p53 acetylation at K120. On one hand, AKT promotes the nuclear entry of Mdm2 and degradation of p53. With increasing AKT*, more Mdm2* is produced to

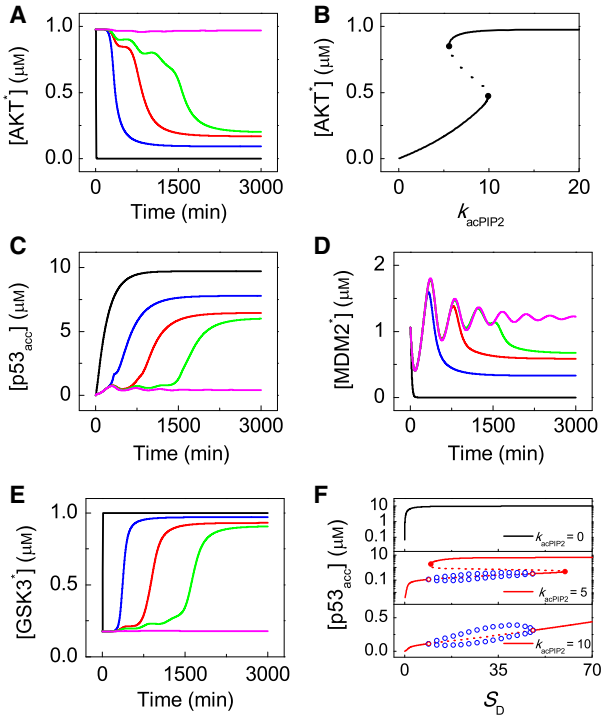

Fig. 5. AKT negatively regulates p53 acetylation on K120. (A, C–E) At S_D = 65, time courses of [AKT*] (A), [$p53_{acc}$] (C), [Mdm2*] (D) and [GSK3*] (E) for k_{acPIP2} = 0 (black), 3 (blue), 5 (red), 5.7 (green) and 10 (magenta). (B) Steady-state level of [AKT*] as a function of k_{acPIP2} for S_D = 65. (F) Steady-state level of [$p53_{acc}$] as a function of S_D for k_{acPIP2} = 0, 5 and 10 (from upper to bottom). The stable and unstable steady states are denoted by solid and dashed lines, respectively. The solid and open circles denote the saddle-node and Hopf bifurcation points, respectively.

degrade p53, delaying or inhibiting the accumulation of $p53_{acc}$ (Fig. 5D). On the other hand, AKT deactivates GSK3 by phosphorylation. The accumulation of active GSK3 is delayed or blocked with increasing AKT*, repressing p53 acetylation directly (Fig. 5E). The basal expression of $p53_{acc}$ is accompanied by GSK3* at basal levels for k_{acPIP2} = 10, suggesting that activation of GSK3 is a prerequisite for high expression of $p53_{acc}$.

The bifurcation diagrams of [$p53_{acc}$] versus S_D for different k_{acPIP2} reveal how $p53_{acc}$ expression is affected by the strength of DNA damage and AKT* abundance (Fig. 5F). [$p53_{acc}$] can undergo a bistable switch with varying S_D for k_{acPIP2} = 5. [$p53_{acc}$] switches to the on state only when S_D is larger than the threshold defined by the right saddle-node bifurcation point. This threshold rises and even disappears with increasing k_{acPIP2}. Consequently, when S_D is fixed at 65, [$p53_{acc}$] switches to the on state more slowly with increasing k_{acPIP2}, and remains in the low-level state for k_{acPIP2} = 10 (see also Fig. 5C). Our results are consistent with the experimental observation that inhibition of AKT activity by PI3K inhibitors promotes apoptosis [11].

p53-induced PTEN inhibits AKT activity and promotes apoptosis

We have shown the role of AKT in promoting cell survival by repressing p53 acetylation. Experimentally, addition of PI3K inhibitor LY294002 elevated the expression of PUMA upon irradiation in U2OS cells [11]. There may exist an intrinsic mechanism for AKT repression in cells, that is, p53-induced PTEN can effectively inhibit AKT activation *via* the p53-PTEN-AKT-Mdm2 PFL [31]. The effects of PTEN on p53 acetylation and apoptosis induction are explored in the following.

Upon severe damage, [PTEN] rises to a high level due to the induction by $p53_{acf}$ and $p53_{acc}$ while [AKT*] drops to a much lower level (Fig. 6A). This anti-correlation suggests that PTEN is required for the inhibition of AKT activity upon lethal damage. To evaluate the influence of PTEN upregulation on PUMA induction, we plot the bifurcation diagram of [PUMA] versus S_D with varying k_{spten} (the rate constant for p53-inducible *pten* expression) (Fig. 6B). Increasing k_{spten} leads to a considerable decrease in the threshold of S_D for PUMA induction. Thus, upregulating PTEN expression makes cells sensitive to DNA damage. On the other hand, when PTEN expression is deficient at k_{spten} = 0.015, [PUMA] cannot be driven to high levels any more. Therefore, enough expression of PTEN by p53 is required for PUMA-induced apoptosis.

The two-parameter bifurcation diagram of S_D versus k_{spten} reveals the effect of PTEN on p53-mediated cell-fate decision (Fig. 6C). The boundary between cell survival and death just corresponds to the thresholds for apoptosis induction. Notably, increasing k_{spten} can improve the cellular sensitivity to DNA damage. The results above indicate that competition between AKT and PTEN affects cellular output markedly. As seen in Fig. 6D, with increasing k_{acPIP2}, more PTEN is required to overcome the inhibitory effect of AKT on apoptosis induction. Collectively, a balance between PTEN and AKT* expression is critical for the proper cellular outcome.

Effects of GSK3-Tip60 cascade on p53-mediated apoptosis

It has been established that active GSK3 activates Tip60 by phosphorylation, and active Tip60 acetylates

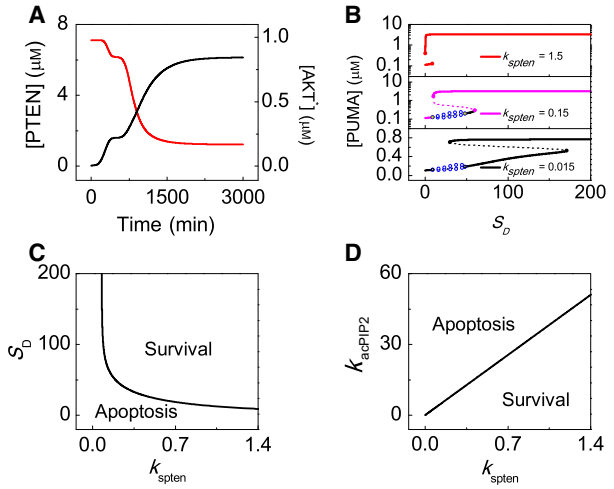

Fig. 6. PTEN is induced by $p53_{acc}$ to repress AKT activation and induce apoptosis. (A) Dynamics of [PTEN] (black) and [AKT*] (red) at $S_D = 65$. (B) Bifurcation diagrams of [PUMA] versus S_D for $k_{spten} = 1.5$ (upper), 0.15 (middle) and 0.015 (bottom). The stable and unstable steady states are denoted by solid and dashed lines, respectively. The solid and open circles denote the saddle-node and Hopf bifurcation points, respectively. (C) Two-parameter bifurcation diagram of S_D and k_{spten}. (D) Two-parameter bifurcation diagram of k_{acPIP2} and k_{spten} with $S_D = 65$.

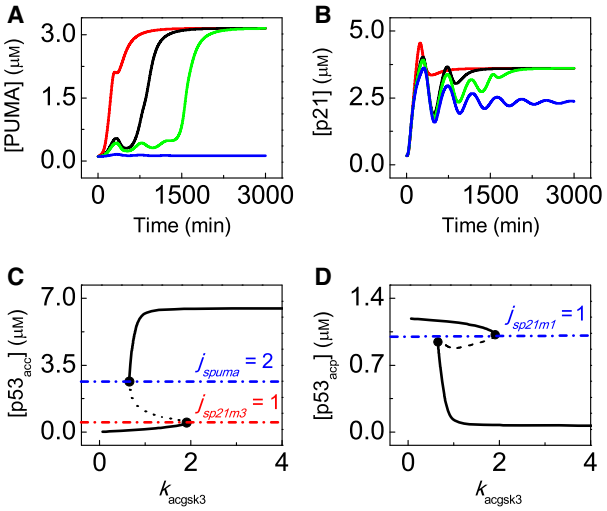

Fig. 7. GSK3 activation is required for p53-dependent apoptosis. (A,B) Time courses of [PUMA] (A) and [p21] (B) at $S_D = 65$ for $k_{acgsk3} = 3$ (red), 2 (black), 1.85 (green) and 1 (blue). (C,D) Steady-state values of [$p53_{acc}$] (C) and [$p53_{acp}$] (D) versus k_{acgsk3} at $S_D = 65$. The threshold of [$p53_{acc}$] and [$p53_{acp}$] for *p21* induction are marked by dash dotted lines.

p53 on K120 to promote apoptosis [10,11]. It is necessary to explore how the GSK3-Tip60 cascade influences the activation of p53 and induction of its target genes.

At $S_D = 65$, the dynamics of [PUMA] vary remarkably for different rate constant of GSK3 activation, k_{acgsk3} (Fig. 7A). Larger k_{acgsk3} accelerates the production of PUMA, whereas [PUMA] remains at basal levels for very small k_{acgsk3}. By contrast, the dynamics of [p21] varies mildly with decreasing k_{acgsk3} (Fig. 7B). Thus, a sufficient amount of active GSK3 is required for the induction of proapoptotic genes instead of proarrest genes, consistent with experimental results that inhibition of GSK3 activity by the inhibitor CT98014 prevents PUMA-dependent apoptosis [11].

The steady-state level of $p53_{acc}$ exhibits bistability over some range of k_{acgsk3}, and the on-state level of $p53_{acc}$ mostly exceeds the threshold for *puma* induction represented by j_{spuma} (Fig. 7C). [$p53_{acc}$] remains in the off state for $k_{acgsk3} < 1.9$, without *puma* induction; otherwise, it switches to the on state. For k_{acgsk3} below the threshold, $p53_{acp}$ is sufficient to induce *p21* since its level is higher than j_{sp21m1} (the threshold of *p21* induction), whereas $p53_{acc}$ takes charge of *p21* induction with k_{acgsk3} above the threshold (Fig. 7C,D). Therefore, sufficient activation of GSK3 is indispensable for *puma* induction, and *p21* can be induced by p53 irrespective of the status of GSK3.

The significance of Tip60 in p53-dependent apoptosis is further investigated. [p21] rises monotonically with $Tip60_{tot}$, while [PUMA] may change as a bistable switch over some range of $Tip60_{tot}$ (Fig. 8A). Neither *p21* nor *puma* can be induced by p53 without Tip60. We further compared the levels of p21 and PUMA at the population level with the experimental data from U2OS cells treated by Tip60 siRNA and 20 μM etoposide [10] (Fig. 8B). Tip60 is required for high induction of both p21 and PUMA, and this is consistent with experimental results [10].

The bifurcation diagrams of steady-state levels of PUMA and p21 versus the activation rate of Tip60, $k_{actip60}$, reveal the role of Tip60 activation in the induction of p53-targeted genes (Fig. 8C). [p21] always stays at high levels even with $k_{actip60} = 0$, whereas PUMA is induced only when $k_{actip60}$ exceeds some threshold. That is, sufficient Tip60 activation is indispensable for PUMA induction instead for p21 induction. To compare our results with the experimental data on the regulation of Tip60 activity by treating U2OS cells with GSK3 and PI3K inhibitors, the activation rate of GSK3 and the rate of PIP3 activation are set to 0 (Fig. 8D). The simulation results show good agreements with experimental data in all the four cases. In fact, the steady-state property of [PUMA] results from the bistable switching of [$p53_{acc}$] with varying $k_{actip60}$. p53 is highly acetylated at K120 only when $k_{actip60}$ is larger than the threshold (Fig. 8E). The dynamics of [$p53_{acc}$] indeed depend remarkably on $k_{actip60}$ (Fig. 8F).

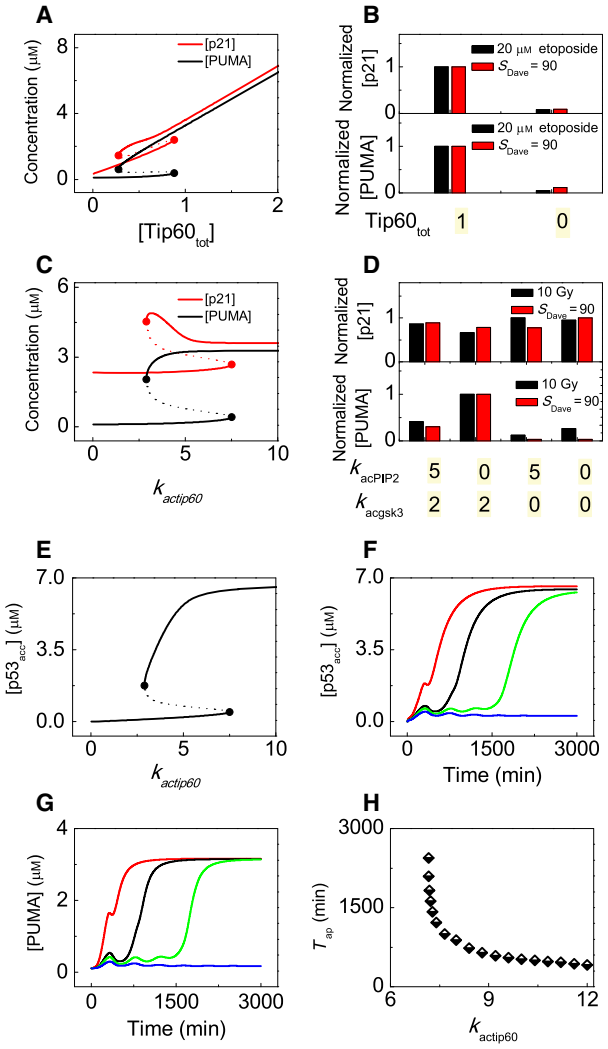

Fig. 8. Tip60 activation specifically induces p53-dependent apoptosis. (A) Bifurcation diagram of [p21] and [PUMA] versus $Tip60_{tot}$. (B) Comparison of the normalized [p21] and [PUMA] in the presence or absence of Tip60. The black histograms denote experimental data from U2OS cells exposed to 20 μM etoposide with Tip60 siRNA (Left black) or control case (Right black) at 6 h [10], and the red ones present the simulation results for $S_{Dave} = 90$ with $Tip60_{tot} = 1$ or 0 as indicated in the bottom. (C) Bifurcation diagrams of [p21] and [PUMA] versus $k_{actip60}$ (the rate constant of Tip60 activation). (D) Comparison of the normalized [p21] and [PUMA] for different cases of adding PI3K or GSK3 inhibitor. The black histograms denote the experimental data from U2OS cells exposed to 10 Gy of γ-irradiation and treated with or without GSK3 inhibitor in the presence or the absence of PI3K inhibitor at 6 h [11]. The red ones stand for the simulation results for different setting of k_{acPIP2} and k_{acgsk3} as indicated in the bottom. $k_{acPIP2} = 0$ and $k_{acgsk3} = 0$ is used to mimic the addition of PI3K inhibitor and GSK3 inhibitor. (C) Bifurcation diagram of $[p53_{acc}]$ versus $k_{actip60}$. (F,G) Time courses of $[p53_{acc}]$ (F) and [PUMA] (G) with $k_{actip60} = 6$, 7.2, 8 and 12 from right to left. (H) The curve of the apoptotic time, T_{ap}, versus $Tip60_{tot}$. S_D is fixed at 65.

$[p53_{acc}]$ switches on more quickly with larger $k_{actip60}$. As a result, PUMA induction accelerates with increasing $k_{actip60}$, that is, apoptosis progression advances with enhanced Tip60 activation (Fig. 8G). To quantify the effect of $k_{actip60}$ on apoptosis induction, we calculated the time required for $[p53_{acc}]$ to exceed its threshold for *puma* induction, that is, T_{ap} (Fig. 8H). T_{ap} rises with reducing $k_{actip60}$ and becomes very large when $k_{actip60}$ approaches the threshold for switching on PUMA. Together, Tip60-mediated p53 acetylation at K120 is required for apoptosis specifically.

Discussion and Conclusion

We have clarified how the dynamics and modifications of p53 mediate the cellular response to DNA damage and elucidated how Tip60-mediated p53 acetylation is dynamically regulated. Tip60 activity is tightly controlled, involving the p53-PTEN-Akt-GSK3-Tip60 PFL. Upon mild damage, Tip60 activity is repressed by AKT, and primarily activated p53 only induces p21 to arrest the cell cycle. Upon severe damage, Tip60 is activated by GSK3, and p53 acetylated on K120 induces PUMA to trigger apoptosis. p53 shows distinct dynamics in the two cases. Such an elegant regulation grantees a precise cell fate decision upon DNA damage.

Tip60 is involved in multiple physiological processes including detection of DNA damage, DNA repair, transcriptional activation and apoptosis induction [32–34]. Here, we focused on its role in apoptosis induction through its acetyltransferase activity. Cell-cycle arrest and apoptosis are selectively induced, depending on the level and acetylation status of p53. Tip60 may act as a co-activator for p53-inducible *p21* expression [10]. The acetyltransferase activity of Tip60 seems irrelevant to *p21* induction since *p21* expression remains unchanged in the case of Tip60 mutation [11]. In addition, we assumed that p53 phosphorylation at Ser46 promotes *pten* induction that facilitates p53 acetylation at K120 by Tip60 [26]. Whether there exists some direct link between *pten* induction and p53 acetylation at K120 is to be identified.

The current model could be extended by characterizing the intricate roles of Tip60 in the DDR. It was reported that Tip60 is indispensable for ATM activation in Hela cells exposed to IR [32]. ATM activation by Tip60-mediated acetylation is not considered in present model. Tip60-mediated ATM activation and DNA repair could be incorporated into the model when more data are available [33]. Tip60 is also a target of E3 ubiquitin ligase Mdm2. Considering Mdm2-mediated degradation of Tip60 could enrich the regulation of Tip60

activity [35]. Specifically, potential competition between p53 and Tip60 for binding to Mdm2 could affect p53 stabilization [34]. It is challenging to develop a more comprehensive model of the DDR involving more functions and regulation of Tip60 in the future.

In our model, the acetyltransferase activity of Tip60 is activated by GSK3-controlled phosphorylation on Ser86. Phosphorylation of Tip60 at T158 by p38α also enables Tip60 to acetylate p53 at K120 [36]. That is, cells can exploit two pathways to regulate Tip60 activity. Indeed, the GSK3-Tip60 and p38α-Tip60 pathway coexist in U2OS cells and can be activated simultaneously under gamma irradiation [11,36]. A plausible explanation is that Tip60 is a very important tumor suppressor, and the existence of multiple activation sites confers it robustness to mutations. It is intriguing to explore whether there exists any interplay between the two pathways in the p53-mediated DDR.

Of note, similar to Tip60, Monocytic Leukemia Zinc Finger (MOZ) can also acetylate p53 at K120 [37]. Similarly, the MOZ-mediated acetylation of p53 is also interfered by pro-survival AKT that phosphorylates MOZ at T369 to block its interaction with PML and p53. More than two pathways are involved in K120 acetylation of p53 and the survival-death competition between p53 and AKT, suggesting the significance and complexity of acetylation modification in p53-mediated cell fate decision. The choice of which or both pathway(s) to exert this modification may be cell type specific. For example, the MOZ pathway seems to be invalid in U2OS cells in which PUMA induction is almost totally impaired when the acetyltransferase activity of Tip60 is inhibited by treating cells with GSK3 inhibitor-CT98014 [11]. Additionally, the novel finding revealed that MOZ could acetylate p53 at K120 and K382 simultaneously [37]. Thus, MOZ may integrate the functions of both Tip60 and p300 in the regulation of p53 acetylation. It is intriguing to explore how these acetyltransferases coordinate to regulate p53 acetylation in the future.

Acknowledgement

This work was supported by the National Natural Science Foundation of China (Nos. 11574139 and 31361163003) and the Fundamental Research Funds for the Central Universities (Nos. 14380013 and 14380015).

Author contributions

X-PZ, FL and WW conceived the project. X-PZ, PW and HB developed the mathematical model. PW and HB performed the simulation and analysis. X-PZ, FL and WW contributed computation and analysis tools. PW, X-PZ and FL wrote the paper. PW, X-PZ and FL revised the paper. PW, X-PZ, FL and WW participated in discussion.

References

1 Vousden KH and Lane DP (2007) p53 in health and disease. *Nat Rev Mol Cell Biol* **8**, 275–283.
2 Haupt Y, Maya R, Kazaz A and Oren M (1997) Mdm2 promotes the rapid degradation of p53. *Nature* **387**, 296–299.
3 Kruse JP and Gu W (2009) Modes of p53 regulation. *Cell* **137**, 609–622.
4 Saito S, Goodarzi AA, Higashimoto Y, Noda Y, Lees-Miller SP, Appella E and Anderson CW (2002) ATM mediates phosphorylation at multiple p53 sites, including Ser46, in response to ionizing radiation. *J Biol Chem* **277**, 12491–12494.
5 Okamura S, Arakawa H, Tanaka T, Nakanishi H, Ng CC, Taya Y, Monden M and Nakamura Y (2001) p53DINP1, a p53-inducible gene, regulates p53-dependent apoptosis. *Mol Cell* **8**, 85–94.
6 Sakaguchi K, Herrera JE, Saito S, Miki T, Bustin M, Vassilev A, Anderson CW and Appella E (1998) DNA damage activates p53 through a phosphorylation-acetylation cascade. *Gene Dev* **12**, 2831–2841.
7 Hofmann TG, Moller A, Sirma H, Zentgraf H, Taya Y, Droge W, Will H and Schmitz ML (2002) Regulation of p53 activity by its interaction with homeodomain-interacting protein kinase-2. *Nat Cell Biol* **4**, 1–10.
8 Tang Y, Zhao W, Chen Y, Zhao Y and Gu W (2008) Acetylation is indispensable for p53 activation. *Cell* **133**, 612–626.
9 Sykes SM, Mellert HS, Holbert MA, Li K, Marmorstein R, Lane WS and McMahon SB (2006) Acetylation of the p53 DNA-binding domain regulates apoptosis induction. *Mol Cell* **24**, 841–851.
10 Tang Y, Luo J, Zhang W and Gu W (2006) Tip60-dependent acetylation of p53 modulates the decision between cell-cycle arrest and apoptosis. *Mol Cell* **24**, 827–839.
11 Charvet C, Wissler M, Brauns-Schubert P, Wang SJ, Tang Y, Sigloch FC, Mellert H, Brandenburg M, Lindner SE, Breit B *et al.* (2011) Phosphorylation of Tip60 by GSK-3 determines the induction of PUMA and apoptosis by p53. *Mol Cell* **42**, 584–596.
12 Cross DA, Alessi DR, Cohen P, Andjelkovich M and Hemmings BA (1995) Inhibition of glycogen synthase kinase-3 by insulin mediated by protein kinase B. *Nature* **378**, 785–789.
13 Batchelor E, Loewer A, Mock C and Lahav G (2011) Stimulus-dependent dynamics of p53 in single cells. *Mol Syst Biol* **7**, 488.

14 Purvis JE, Karhohs KW, Mock C, Batchelor E, Loewer A and Lahav G (2012) p53 dynamics control cell fate. *Science* **336**, 1440–1444.
15 Chen X, Chen J, Gan S, Guan H, Zhou Y, Ouyang Q and Shi J (2013) DNA damage strength modulates a bimodal switch of p53 dynamics for cell-fate control. *BMC Biol* **11** (1), 73.
16 Wee KB and Aguda BD (2006) Akt versus p53 in a network of oncogenes and tumor suppressor genes regulating cell survival and death. *Biophys J* **91**, 857–865.
17 Zhang T, Brazhnik P and Tyson JJ (2007) Exploring mechanisms of the DNA-damage response: p53 pulses and their possible relevance to apoptosis. *Cell Cycle* **6**, 85–94.
18 Zhang XP, Liu F, Cheng Z and Wang W (2009) Cell fate decision mediated by p53 pulses. *Proc Natl Acad Sci USA* **106**, 12245–12250.
19 Zhang XP, Liu F and Wang W (2011) Two-phase dynamics of p53 in the DNA damage response. *Proc Natl Acad Sci USA* **108**, 8990–8995.
20 Hat B, Kochańczyk M, Bogdał MN and Lipniacki T (2016) Feedbacks, bifurcations, and cell fate decision-making in the p53 system. *PLoS Comput Biol* **12**, e1004787.
21 Mayo LD and Donner DB (2001) A phosphatidylinositol 3-kinase/Akt pathway promotes translocation of Mdm2 from the cytoplasm to the nucleus. *Proc Natl Acad Sci USA* **98**, 11598–11603.
22 Prives C (1998) Signaling to p53: breaking the MDM2-p53 circuit. *Cell* **95**, 5–8.
23 Demonacos C, Krstic-Demonacos M, Smith L, Xu D, O'Connor DP, Jansson M and La Thangue NB (2004) A new effector pathway links ATM kinase with the DNA damage response. *Nat Cell Biol* **6**, 968.
24 Smith L and Thangue NBL (2005) Signalling DNA damage by regulating p53 co-factor activity. *Cell Cycle* **4**, 30–32.
25 Batchelor E, Mock CS, Bhan I, Loewer A and Lahav G (2008) Recurrent initiation: a mechanism for triggering p53 pulses in response to DNA damage. *Mol Cell* **30**, 277–289.
26 Mayo LD, Seo YR, Jackson MW, Smith ML, Guzman JR, Korgaonkar CK and Donner DB (2005) Phosphorylation of human p53 at serine 46 determines promoter selection and whether apoptosis is attenuated or amplified. *J Biol Chem* **280**, 25953–25959.
27 Mayo LD and Donner DB (2002) The PTEN, Mdm2, p53 tumor suppressor–oncoprotein network. *Trends Biochem Sci* **27**, 462–467.
28 Gottlieb TM, Leal JFM, Seger R, Taya Y and Oren M (2002) Cross-talk between Akt, p53 and Mdm2: possible implications for the regulation of apoptosis. *Oncogene* **21**, 1299–1303.
29 Weinberg RL, Veprintsev DB, Bycroft M and Fersht AR (2005) Comparative binding of p53 to its promoter and DNA recognition elements. *J Mol Biol* **348**, 589–596.
30 Wu M, Ye H, Tang Z, Shao C, Lu G, Chen B, Yang Y, Wang G and Hao H (2017) p53 dynamics orchestrates with binding affinity to target genes for cell fate decision. *Cell Death Dis* **8**, e3130.
31 Mayo LD, Dixon JE, Durden DL, Tonks NK and Donner DB (2002) PTEN protects p53 from Mdm2 and sensitizes cancer cells to chemotherapy. *J Biol Chem* **277**, 5484–5489.
32 Sun Y, Jiang X, Chen S, Fernandes N and Price BD (2005) A role for the Tip60 histone acetyltransferase in the acetylation and activation of ATM. *Proc Natl Acad Sci USA* **102**, 13182–13187.
33 Ikura T, Ogryzko VV, Grigoriev M, Groisman R, Wang J, Horikoshi M, Scully R, Qin J and Nakatani Y (2000) Involvement of the TIP60 histone acetylase complex in DNA repair and apoptosis. *Cell* **102**, 463–473.
34 Legube G, Linares LK, Tyteca S, Caron C, Scheffner M, Chevillard-Briet M and Trouche D (2004) Role of the histone acetyl transferase Tip60 in the p53 pathway. *J Biol Chem* **279**, 44825–44833.
35 Legube G, Linares LK, Lemercier C, Scheffner M, Khochbin S and Trouche D (2002) Tip60 is targeted to proteasome-mediated degradation by Mdm2 and accumulates after UV irradiation. *EMBO J* **21**, 1704–1712.
36 Xu Y, Liao R, Li N, Xiang R and Sun P (2014) Phosphorylation of Tip60 by p38α regulates p53-mediated PUMA induction and apoptosis in response to DNA damage. *Oncotarget* **5**, 12555–12572.
37 Rokudai S, Laptenko O, Arnal SM, Taya Y, Kitabayashi I and Prives C (2013) MOZ increases p53 acetylation and premature senescence through its complex formation with PML. *Proc Natl Acad Sci USA* **110**, 3895–3900.

Supporting information

Additional supporting information may be found online in the Supporting Information section at the end of the article.
Method S1. Equations of the model.
Table S1. Description and initial values of variables.
Table S2. Parameters of the model.